



OPEN

Quantitative Analysis of Enhancement Intensity and Patterns on Contrast-enhanced Spectral Mammography

Ying Liu^{1,2}, Shuang Zhao^{1,2}, Juan Huang¹, Xueqin Zhang¹, Yun Qin¹, Huanhuan Zhong¹ & Jianqun Yu¹

CESM is an emerging digital mammography technology with a high breast cancer detection and a limited diagnostic specificity. In order to improve specificity, we quantitatively assessed enhancement intensity of breast lesions with different pathological types and hormonal receptor status and evaluated the consistency of enhancement patterns between CESM and DCE-MRI. A total of 145 lesions were enrolled, consisting of 43 malignant (17 non-infiltrating cancers and 26 infiltrating cancers) and 99 benign lesions. The diagnostic performance of enhancement intensity in the former positions was significantly higher than that in the latter positions (AUC: 0.834 vs. 0.755, $p = 0.0008$). Infiltrating cancers showed the highest enhancement intensity, while benign lesions the lowest (mean CNR_1 : 7.6% vs. 2.7%; median CNR_1 : 6.8% vs. 2.7%). Enhancement intensity of ER or PR positive group was weaker than negative group, while HER-2 positive group was stronger than negative group. 28 patients with 28 lesions performed both CESM and DCE-MRI examinations, showing a coincidence rate of 64.2% and moderate agreement ($k = 0.515$) between CESM and DCE-MRI. In conclusion, quantitative analysis of enhancement characteristics is feasible to the diagnosis practice on CESM.

Breast cancer is the most common malignant tumor in women around the world¹. Although mammography is generally considered the preferred screening method for breast cancer and can substantially reduce breast cancer mortality, its diagnostic performance is affected by mammary gland density and the sensitivity decreases significantly in dense breasts².

Contrast-enhanced spectral mammography (CESM), an emerging digital mammography technology, has been approved by the U.S. FDA and put into clinical use in 2011. After intravenous iodine contrast agent, pairs of low-energy (LE) and high-energy images are acquired to generate the subtraction images. LE and subtraction images are applied to the diagnostic procedure. LE images are similar to full-field digital mammography (FFDM)³, which can clearly demonstrate the morphological features of breast lesions. On the basis of angiogenesis, breast lesions reveal enhancement and are highlighted on subtraction images by eliminating overlapping of breast fibroglandular tissues^{4–6}. Accordingly, CESM dramatically improves the cancer detection and decreases the misdiagnosis rate, especially in dense breasts^{7–10}.

Given that a number of benign lesions can reveal enhancement on CESM^{8,11}, researchers have focused on how to differentiate breast cancers from benign lesions and improve the diagnostic specificity. Previous studies^{12–14} have proved the diagnostic performance of enhancement intensity for breast cancers and concluded that enhancement intensity of malignancies was usually stronger than that of benign lesions. Moreover, invasive cancers were inclined to enhance stronger than non-invasive cancers and benign lesions^{12,14}. However, there is no research before investigating the correlation between enhancement intensity and hormonal receptor status of breast cancers. As for enhancement patterns, several published papers^{4,13,15} claimed that the distribution of enhancement patterns between benign and malignant lesions was different, which was similar to time-intensity curve (TIC) on breast dynamic contrast-enhanced magnetic resonance imaging (DCE-MRI). Whereas, it is uncertain that how is the agreement between two modalities. This study was aim to quantitatively assess enhancement intensity of

¹Department of Radiology, Sichuan University West China Hospital, No. 37 Guoxue Alley, Chengdu, 610041, Sichuan Province, China. ²These authors contributed equally: Ying Liu and Shuang Zhao. ✉e-mail: cj.yujianqun@vip.163.com

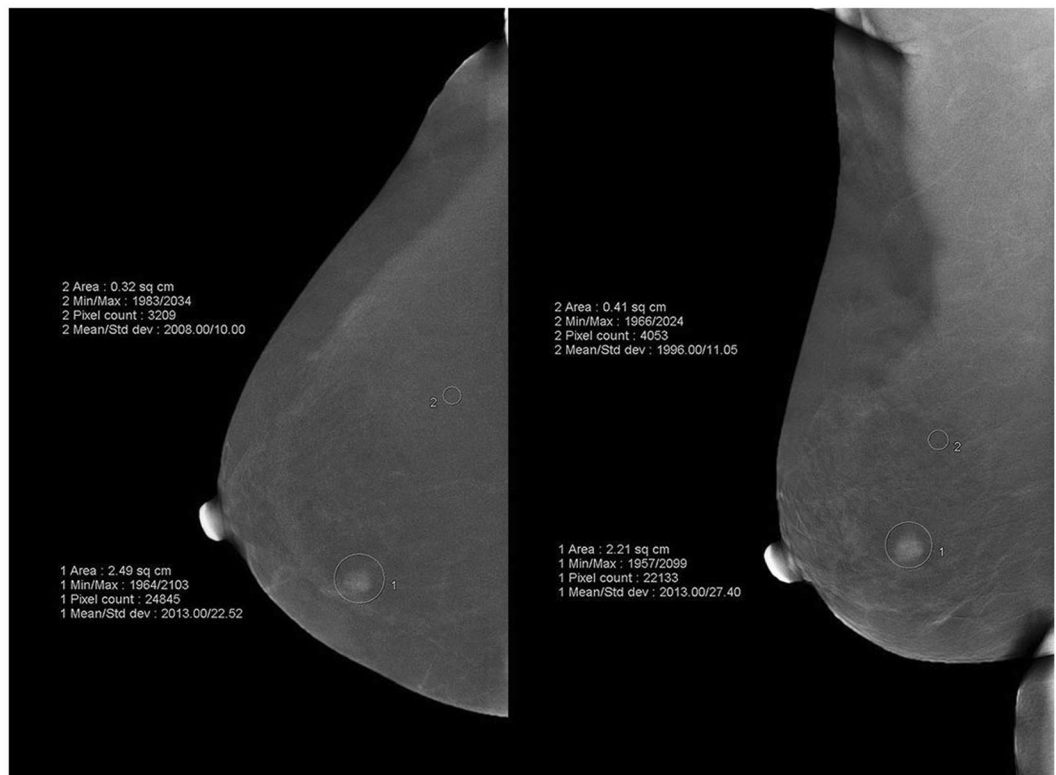


Figure 1. Illustration of quantitative measurements of breast lesions and background. ROIs of breast lesions should cover the entire enhanced areas and ROIs of background were as close as possible to the fatty background components of the breast and away from the enhanced lesion or enhanced breast parenchyma tissues.

breast lesions with different pathological types and hormonal receptor status on CEM and evaluate the consistency of enhancement patterns between CEM and DCE-MRI.

Methods

Patients. The ethical committee of West China Hospital approved this retrospective study with a waiver of informed consent (20/08/2019, NO. 737 2019). All methods were performed in accordance with the relevant guidelines and regulations. CEM was performed on patients with clinically or ultrasonically suspected breast lesions from July 2017 to April 2019. Criteria for selecting the subjects were as follows: more than 18 years old; obtained pathological diagnosis after CEM and DCE-MRI examinations. Samples were excluded from the research if they were: pregnant or breastfeeding; had contraindications to contrast agent, such as renal dysfunction or contrast agent allergy; had a history of hormone treatment or radiation therapy or neoadjuvant chemotherapy for breast lesions before CEM examination. All patients were followed up for more than 6 months.

CEM. CEM was performed using a GE healthcare equipment (SenoBright®). Detailed procedures have been provided elsewhere¹⁶. After intravenous iodine contrast agent (300 mg iodine/ml, 1.5 ml/kg body weight, flow rate 3 ml/s) for about two minutes, a series of consecutive images were acquired including standard craniocaudal (CC) and mediolateral oblique (MLO) views with breast compressed. The process of image acquisition was carried out in five minutes. For one projective position, a pair of low- and high-energy exposures was performed within 1.5 s and a subtraction image was obtained using a special algorithm. For bilateral breasts in two separate views, LE images (similar to FFDM) and subtraction images (which can reveal enhanced area clearly), can be utilized for diagnosis on the workstation.

On subtraction images, a positive finding referred to an enhancement region stronger than background parenchyma enhancement. A region of interest (ROI) was drawn artificially by one radiologist, and then contrast-to-noise ratio (CNR) was measured to assess enhancement intensity and relative signal difference (RSD) was calculated to value enhancement pattern. ROIs of breast lesions should cover the entire enhanced areas and ROIs of background were as close as possible to the fatty background components of the breast and away from the enhanced lesion or enhanced breast parenchyma tissues (Fig. 1). CNR reflected the signal difference between the enhanced lesion and background. CNR values of one index lesion in two projective views were calculated respectively according to time sequence. We defined CNR_1 as the enhancement intensity in the former position, which is a relatively early phase. And CNR_2 represented the enhancement intensity in the latter position, which is a relatively late phase. The specific calculation formulas are listed as follows:

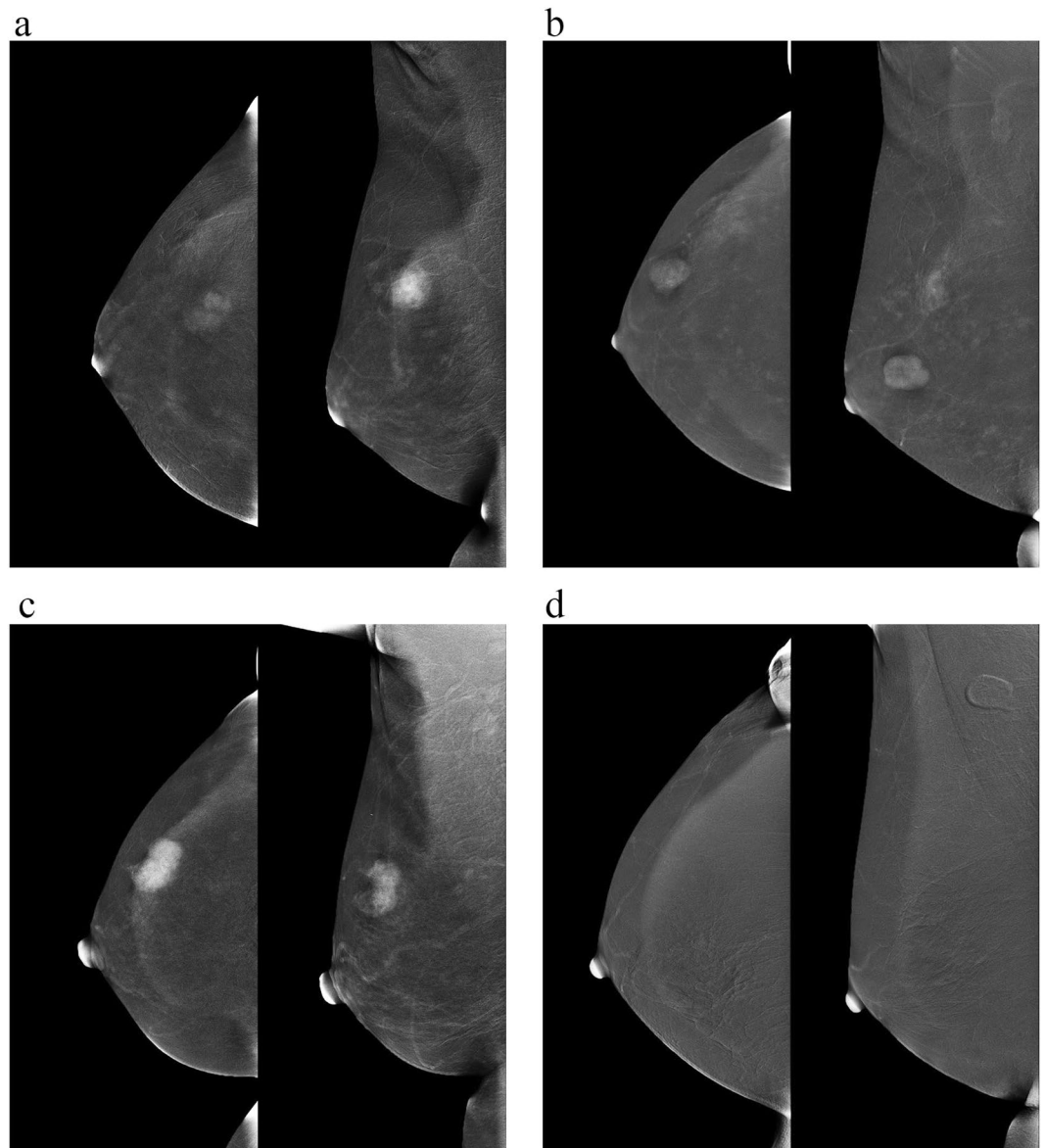


Figure 2. Four different enhancement patterns on CESM. According to RSD values, enhancement patterns were classified as (a) ascending pattern, (b) steady pattern, (c) descending pattern and (d) no enhancement.

$$\text{CNR} = \frac{\text{Sa} - \text{Sb}}{\text{Sb}}$$

Sa: maximum pixel value in ROI of breast lesion
Sb: mean pixel value signal in ROI of background

$$\text{RSD} = \frac{\text{CNR}_2 - \text{CNR}_1}{\text{CNR}_1} \times 100\%$$

CNR₁: CNR value in the former projection
CNR₂: CNR value in the latter projection

On subtraction image, CNR or RSD value of a non-enhanced lesion was scored as zero. According to the changes of CNR values between the former and latter projections, enhancement patterns were classified as four types: ascending pattern, steady pattern, descending pattern and no enhancement (Fig. 2). Ascending pattern: the enhancement intensity showed a continuous rising state with the RSD > 10%. Steady pattern: the enhancement intensity displayed no noticeable difference between the two projections with the absolute value of RSD ≤ 10%. Descending pattern: the enhancement intensity in the latter position is weaker than the former one with RSD < -10%.

DCE-MRI. MRI and CESM examinations were scheduled within one month. The breast MRI study was conducted on the 3.0 T imaging system (Discovery MR750W, GE Healthcare, Chalfont St. Giles, UK) with dedicated bilateral breast-surface coils. Patients were in prone position and T1- and fat-suppressed T2-weighted imaging and diffusion-weighted imaging were acquired before contrast. After intravenous gadolinium (0.2 ml/kg body weight, flow rate 2 ml/s), a dynamic series of fat-suppressed 3-dimensional T1-weighted images were collected. Based on the 5th edition of Breast Imaging Reporting and Data System (BI-RADS), TICs were categorized as persistent, plateau, or washout types.

Histopathology. Pathological specimens were obtained by biopsy or surgical excision. Pathological classification and hormonal receptor status, including estrogen receptor (ER), progesterone receptor (PR) and human epidermal growth factor receptor-2 (HER-2), were recorded. According to immunohistochemistry (IHC), nuclear staining $\geq 10\%$ was regarded as positive for ER and PR status. Expression of HER-2 protein was classified as 0, 1+, 2+, and 3+ by IHC. If a specimen was categorized as 2+, fluorescence *in situ* hybridization (FISH) was performed to test HER-2 gene. HER-2 positivity was defined as an IHC HER-2 score of 3+ or gene amplification by FISH. HER-2 negativity was defined as an IHC HER-2 score of 0 or 1+.

Statistical analysis. Data analysis was conducted using SPSS Statistics (version 19.0, IBM, Armonk, NY) and MedCalc (version 15.6.1, MedCalc Software, Ostend, Belgium). For non-normal distribution parameters, descriptive statistics were expressed as the mean, median, minimum, maximum, and percentiles. Statistical inference was accomplished by Wilcoxon signed rank test for two relative groups, Mann-Whitney U test for two independent groups and Kruskal–Wallis test for more than two independent groups. Moreover, the Bonferroni method was utilized to adjust for multiple comparisons. The diagnostic performance of the examination was calculated compared to pathological findings. The cut-off values were based on the Youden's J statistics and the diagnostic performances were assessed by analyzing the receiver operating characteristics (ROC) curves of subjects. Cohen's kappa coefficient was calculated to measure the agreement between the CESM and MRI. In all tests, a p -value < 0.05 was deemed significant.

Results

Patients and lesions characteristics. For patients who had undergone CESM, we followed the clinical diagnostic and treatment process for more than 6 months, 145 lesions in 131 female patients were included for analysis. The mean patient age was 42 years (range, 18–77 years). In all, 102/145 (70.3%) were benign lesions and 43/145 (29.7%) were breast cancers. The benign lesions included fibroadenomas ($n = 53$), adenosis with or without fibrocystic changes ($n = 33$), intraductal papillomas ($n = 8$), atypical ductal hyperplasia ($n = 3$), usual ductal hyperplasia ($n = 1$), sclerosing adenosis ($n = 1$), inflammation ($n = 1$), duct ectasia ($n = 1$), and cyst ($n = 1$). There were 17 non-infiltrating cancers and 26 infiltrating cancers. These malignant lesions included ductal carcinoma *in situ* ($n = 14$), invasive ductal carcinoma ($n = 23$), solid papillary carcinoma associated with invasive ductal carcinoma ($n = 2$), invasive lobular carcinoma ($n = 1$), lobular carcinoma *in situ* ($n = 1$), mixed ductal carcinoma *in situ* associated and invasive lobular carcinoma ($n = 1$), and invasive adenocarcinoma ($n = 1$).

Of 43 breast cancers, we obtained ER and PR expression characteristics in 41 tumors, and HER-2 expression characteristics in 30 tumors. 30/41 (73.2%) were ER-positive cancers and 11/41 (26.8%) were ER-negative cancers. 24/41 (58.5%) were PR-positive cancers and 17/41 (41.5%) were PR-negative cancers. 9/30 (30.0%) were ER-positive cancers and 21/30 (70.0%) were ER-negative cancers.

CESM findings. LE images depicted 56 lesions, of which 28 were benign lesions and 28 were breast cancers. On subtraction images, 52.9% (54/102) of benign lesions and 97.7% (42/43) of cancers revealed enhancement and can be depicted. Subtraction images failed to show 49 lesions due to no distinguishable enhancement, including 48 benign lesions and 1 ductal carcinoma *in situ* (DCIS). Of 54 enhanced benign lesions, 33 were diagnosed with fibroadenomas, 8 adenosis, and 6 intraductal papillomas, occupying 62.3% (33/53) of fibroadenomas, 24.2% (8/33) of adenosis, and 75.0% (6/8) of intraductal papillomas, separately. Other pathologic entities can also present as enhancement, but just account for a small percentage. In all 145 lesions, 49 only be found on subtraction images, but showed no visible abnormality on LE images, consisting of 15 malignancies and 34 benign lesions. However, 8 benign lesions and 1 DCIS only be detected on LE mammograms and can't be observed on subtraction images. 40 lesions displayed no obvious abnormalities on both LE and subtraction mammograms, which were all proved to be benign. And 47 lesions (20 benign lesions and 27 breast cancer) can be detected by both examinations.

Enhancement intensity on CESM. Table 1 provides the descriptive results of CNR values in different pathological diseases. In terms of the mean, median, maximum, and percentiles, enhancement intensity of breast cancers was significantly higher than that of benign lesions. Both CNR_1 and CNR_2 values of the three groups differed significantly ($p < 0.001$; $p < 0.001$). After the Bonferroni correction, the distribution of CNR_1 values in benign lesions and non-infiltrating cancers ($p = 0.001$), and in benign lesions and infiltrating cancers ($p < 0.001$), was statistically significant, while the difference between non-infiltrating cancers and infiltrating cancers was not statistically significant ($p = 1.000$). The distribution of CNR_2 values in benign lesions and non-infiltrating cancers ($p < 0.001$), and in benign lesions and infiltrating cancers ($p < 0.001$), was statistically significant, while the difference between non-infiltrating cancers and infiltrating cancers was not statistically significant ($p = 1.000$). For benign group, enhancement intensity in latter position was stronger than in former position ($p = 0.028$). Mean CNR_1 was 2.7%, mean CNR_2 was 3.0%, median CNR_1 was 2.7%, and median CNR_2 was 3.3%. By contrast, for breast cancers, enhancement intensity in latter position was weaker compared to former position (non-infiltrating cancers, $p = 0.301$; infiltrating cancers, $p = 0.006$). In non-infiltrating group, mean CNR_1 was 6.5%, mean CNR_2

CNR Values	Benign Lesions (n = 102)		Non-infiltrating Cancers (n = 17)		Infiltrating Cancers (n = 26)		
	Former Position	Latter Position	Former Position	Latter Position	Former Position	Latter Position	
Mean	2.7%	3.0%	6.5%	6.2%	7.6%	6.4%	
Median	2.7%	3.3%	6.8%	5.6%	6.8%	5.6%	
Minimum	0	0	0	0	1.8%	0.6%	
Maximum	10.1%	13.2%	11.8%	10.4%	27.2%	26.0%	
Percentiles	25	0.0%	0.0%	5.0%	4.3%	4.9%	4.3%
	50	2.7%	3.3%	6.8%	5.6%	6.8%	5.6%
	75	4.8%	5.2%	8.1%	8.5%	9.2%	7.5%
<i>p</i> -value	0.028		0.301		0.006		

Table 1. Detailed descriptive results of CNR values of different pathological diseases.

CNR ₁ Values	ER Status (n = 41)		PR Status (n = 41)		HER-2 Status (n = 30)		
	Positive (n = 30)	Negative (n = 11)	Positive (n = 24)	Negative (n = 17)	Positive (n = 9)	Negative (n = 21)	
Mean	6.4%	9.7%	6.6%	8.1%	7.6%	6.4%	
Median	5.9%	7.7%	6.2%	7.0%	7.2%	6.7%	
Minimum	0	4.4%	0.0%	3.4%	5.4%	0.0%	
Maximum	11.8%	27.2%	11.8%	27.2%	10.5%	11.8%	
Percentiles	25	4.8%	6.9%	4.8%	5.7%	6.3%	4.6%
	50	5.9%	7.7%	6.2%	7.0%	7.2%	6.7%
	75	8.1%	10.2%	8.9%	8.5%	9.1%	8.2%
<i>p</i> -value	0.037		0.508		0.283		

Table 2. Detailed descriptive results of CNR₁ values of breast cancers with different hormonal receptor status.

RSD values	Benign (n = 102)	Malignant (n = 43)	<i>p</i> -value	
Mean	11.0%	−9.7%	<0.001	
Median	0	−11.9%		
Minimum	−33.1%	−70.8%		
Maximum	215.1%	48.5%		
Percentiles	25	0		−24.4%
	50	0		−11.9%
	75	11.4%		6.0%

Table 3. Detailed descriptive results of RSD values of different pathological diseases.

was 6.2%, median CNR₁ was 6.8%, and median CNR₂ was 5.6%. In infiltrating group, mean CNR₁ was 7.6%, mean CNR₂ was 6.4%, median CNR₁ was 6.8%, and median CNR₂ was 5.6%.

The sensitivities were 81.4% for CNR₁ and 93.0% for CNR₂. The specificities were 75.5% for CNR₁ and 52.9% for CNR₂. The area under the ROC curves (AUCs) were 0.843 (95% confidence interval [CI]: 0.773–0.898; $p < 0.0001$) for CNR₁, and 0.755 (95% CI: 0.677–0.822; $p < 0.0001$) for CNR₂. The AUC was significantly higher for CNR₁ than it was for CNR₂ ($p = 0.0008$).

We used CNR₁ to value enhancement intensity of cancers with different hormonal receptor status (Table 2). Enhancement intensity of ER positive group was weaker than ER negative group ($p = 0.037$). For ER positive and negative cancers, mean CNR₁ was 6.4% vs. 9.7%, and median CNR₁ was 5.9% vs. 7.7%. Enhancement intensity of PR positive group was weaker than PR negative group ($p = 0.508$). For PR positive and negative cancers, mean CNR₁ was 6.6% vs. 8.1%, and median CNR₁ was 6.2% vs. 7.0%. Enhancement intensity of HER-2 positive group was stronger than HER-2 negative group ($p = 0.283$). For HER-2 positive and negative cancers, mean CNR₁ was 7.6% vs. 6.4%, and median CNR₁ was 7.2% vs. 6.7%.

Enhancement patterns on CEM and MRI. Detailed descriptive results of RSD values are listed in Table 3. Mean RSD of benign group was 11.0% and median value was 0, while mean RSD of malignancies was −9.7% and median value was −11.9%. The differences of RSD values between benign and malignant lesions were significant ($p < 0.001$). Enhancement patterns on CEM in different pathological diseases are provided in Table 4. As for benign group, ascending pattern accounted for 25.5% (26/102), steady pattern 16.7% (17/102),

Enhancement patterns	Benign (n = 102)	Malignant (n = 43)	p-value
No enhancement	48 (47.1%)	1 (2.3%)	<0.001
Ascending pattern	26 (25.5%)	8 (18.6%)	
Steady pattern	17 (16.7%)	12 (27.9%)	
Descending pattern	11 (10.8%)	22 (51.2%)	

Table 4. Enhancement patterns on CESM in different pathological diseases. Percentages are in parentheses.

descending pattern 10.8% (11/102), and non-enhanced group 47.1% (48/102). The proportions of enhancement patterns in malignancies were 18.6% (8/43) for ascending pattern, 27.9% (12/43) for steady pattern, 51.2% (22/43) for descending pattern, and 2.3% (1/43) for non-enhanced type. The distribution of enhancement patterns in benign and malignant groups was statistically different ($p < 0.001$).

28 patients with 28 lesions performed both CESM and DCE-MRI examinations. The results of TICs on DCE-MRI are listed as follows: in 12 benign lesions, 33.3% (4/12) without enhancement, 25.0% (3/12) with persistent types, 25.0% (3/12) with plateau types, and 16.7% (2/12) with washout types; in 16 malignant lesions, 12.5% (2/16) with persistent types, 50.0% (8/16) with plateau types, and 37.5% (6/16) with washout types. The distribution of TUCs in benign and malignant groups was statistically different ($p = 0.046$).

Comparing enhancement patterns on CESM and TICs on DCE-MRI, the results demonstrated that 2/28 (7.1%) lesions with a concordant ascending pattern (or persistent type), 5/28 (17.8%) lesions with a concordant steady pattern (or plateau type), 7/28 (25.0%) lesions with a concordant descending pattern (or washout type), 4/28 (14.3%) lesions with no enhancement, and 10/28 (35.7%) lesions with inconsistent enhancement patterns. The coincidence rate of two modalities was 64.2%. Cohen's kappa showed moderate agreement ($k = 0.515$) between CESM and MRI.

For 96 enhanced lesions, an average time gap between the former and latter projections of suspicious breast was 104 seconds (range, 54–227 seconds). Images of CC position were projected prior to MLO position in a large portion of cases (79 lesions), and MLO views were projected prior to CC views in 17 lesions. Among 42 enhanced cancers, 37 lesions projected CC views first and 5 projected MLO views first, respectively, accounting for 21.6% (8/37) and 0 in ascending pattern, 21.6% (8/37) and 80.0% (4/5) in steady pattern, 56.8% (21/37) and 20.0% (1/5) in descending pattern. By contrast, 42 benign lesions projected CC views first and 12 projected MLO views first, respectively, occupying 47.6% (20/42) and 50.0% (6/12) in ascending pattern, 35.7% (15/42) and 16.7% (2/12) in steady pattern, 16.7% (7/42) and 33.3% (4/12) in descending pattern. There was no statistically significant difference in the distribution of enhancement patterns between CC prior to MLO and MLO prior to CC conditions in benign group ($p = 0.304$), while the difference was significant in malignancies ($p = 0.027$).

Discussion

Based on the angiogenesis, breast lesions can be clearly demonstrated on CESM by eliminating the overlapping of breast fibroglandular tissues^{4–6}. CESM is superior to conventional mammography and improves breast cancer detection¹⁰. In this study, CESM demonstrated 97.6% (42/43) of malignancies, while LE only revealed 65.1% (28/43) of cancers, indicating a higher cancer detection rate on CESM. However, we observed that 51.5% (51/102) of benign lesions revealed enhancement on CESM, which means that it is not proper to diagnose the lesions depending on whether it is enhanced or not. In order to explore enhancement characteristics between benign and malignant lesions and improve diagnostic specificity, we conducted this study. We quantitatively assessed enhancement intensity of breast lesions with different pathological types and hormonal receptor status on CESM and evaluated the consistency of enhancement patterns between CESM and DCE-MRI.

For enhancement intensity, this preliminary research suggested that enhancement intensity of malignancies was usually stronger than that of benign lesions (Table 1), which was consistent with other researchers' findings^{6,11–14,17}. Lewin *et al.*⁶ concluded that 84.6% (11/13) of invasive cancers enhanced strongly, while all benign lesions ($n = 12$) were presented as no or weak enhancement qualitatively. Luczynska *et al.*¹⁴ observed medium or strong enhancement among 83% (106/127) invasive carcinomas while no enhancement or weak enhancement among 71% (58/82) benign lesions. Using a quantitative program, Deng *et al.*¹³ reported that the mean pixel value of malignant lesions was 476.05 (versus 85.79 for benign lesions).

Rudnicki *et al.*¹² and our researches took a quantitative method to evaluate enhancement intensity of lesions on the both two projections (CC and MLO views). Rudnicki *et al.* adopted the percentage signal difference between enhancing lesion and background (%RS) to value the intensity of lesions, which was similar to CNR index in this research. The only difference between %RS and CNR was that Rudnicki *et al.* measured mean signals of lesions, whereas we measured maximum signals, which took into consideration that the heterogeneity of lesions may had effect on mean signals and caused unstable results. Both we found that mean %RS and CNR values were correlated with pathological classification. Comparison of three different pathological classifications indicated that infiltrating cancers showed the highest values, while benign lesions the lowest.

In CESM protocols, Rudnicki *et al.* performed CC views prior to MLO views. While the sequence of CC or MLO position was not fixed in this study, CNR_1 was defined to present enhancement intensity in the former projection and CNR_2 to present the latter projection. According to Rudnicki's data, the AUCs were 0.725 in the former projection and 0.713 in the latter projection. They concluded that the difference between two views was not significant and two views had similar diagnostic accuracy, which probably because the time interval between two projections was not long enough. But we came up with different results. We calculated an AUC of 0.843 in the former projection and 0.755 in the latter projection and found a significant difference of enhancement intensity

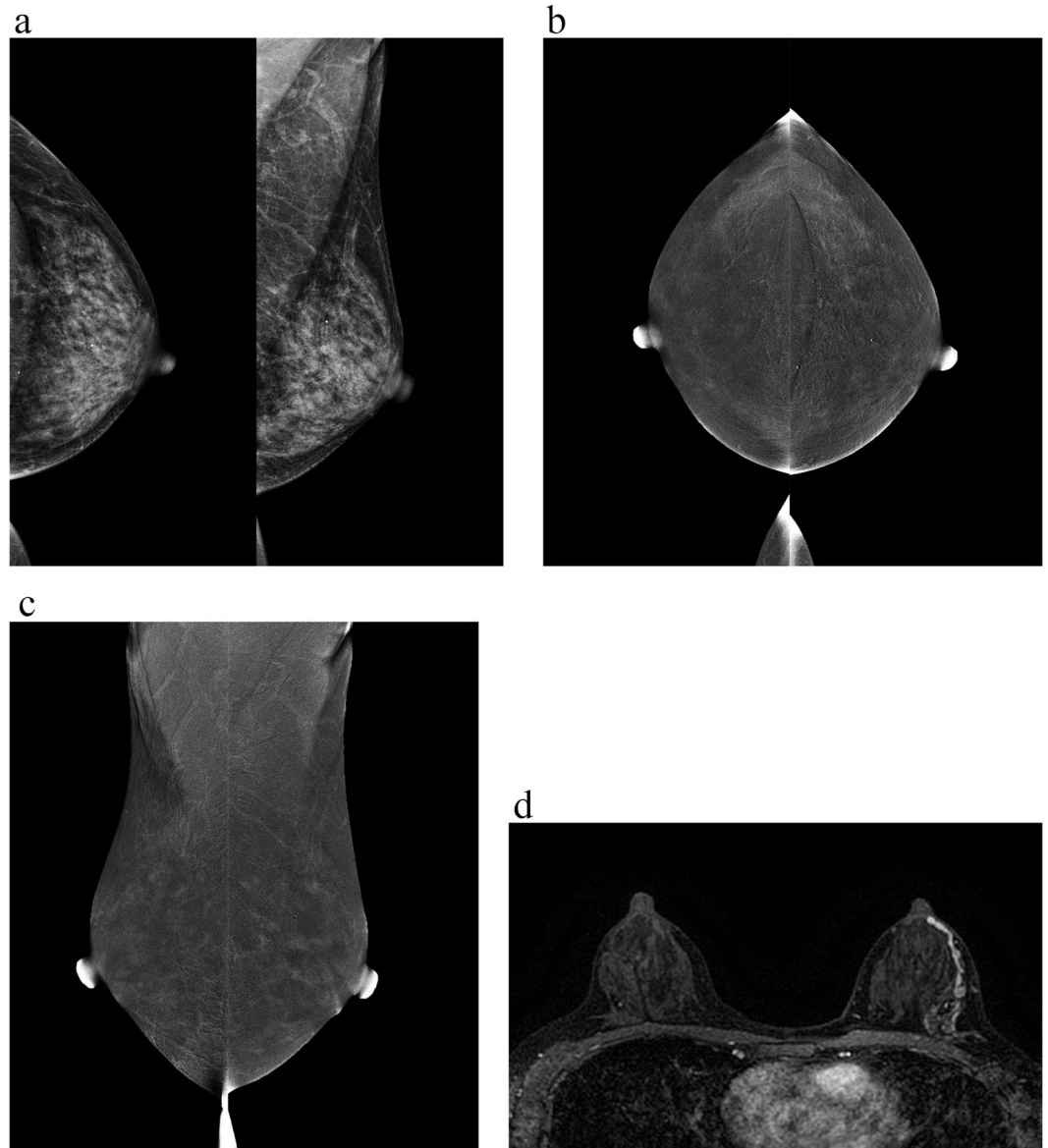


Figure 3. A 47-year-old woman with one ductal carcinoma *in situ* in the left breast at 3 o'clock. **(a)** Low-energy images in CC and MLO views show scattered microcalcifications in the left breast. **(b)** Subtraction images in CC views and **(c)** MLO views display symmetrical moderate background parenchyma enhancement in bilateral breasts and no distinct enhancing areas stronger than background enhancement are detected. **(d)** Contrast-enhanced MRI depicted non-mass enhancement with linear distribution.

between two views, indicating that the former projections of contrast-enhanced images seemed to play a more important role in the diagnosis of breast lesions compared with the latter projective views.

Marino *et al.*¹⁸ had found that CESM and radiomics analysis had differential value in hormonal receptor status with accuracy of 78.4% to 100%. This study analysed CNR differences between receptor positive and negative lesions and concluded that enhancement intensity was related to hormonal receptor status. Enhancement intensity of ER or PR positive group was weaker than negative group and HER-2 positive group was stronger than negative group, of which the signal discrepancy between ER positive and negative lesions was statistically significant. It suggested that CESM may contribute to differentiate hormonal receptor status. Due to insufficient sample size, the results needed further confirmation.

As indicated in Table 1, CNR_2 was lower than CNR_1 in malignant group, while CNR_2 was higher than CNR_1 in benign group, which revealed a significant discrepancy of enhancement intensity between the former and latter projections. According to this, we further investigated enhancement patterns of breast lesions. The classification of enhancement patterns on CESM was similar to the TIC on breast DCE-MRI. On MRI, Kuhl *et al.*¹⁹ showed enhancement types among 101 malignant lesions as follows: persistent enhancement, 8.9%; plateau enhancement, 33.6%; and washout enhancement 57.4%. For 165 benign lesions, results were as follows: persistent enhancement, 83.0%; plateau enhancement, 11.5%; and washout enhancement 5.5%. On CESM, previous studies^{4,13,15}

had described enhancement patterns of breast lesions. Both Jong *et al.*¹⁵ and Dromain *et al.*⁴ took consecutive exposures in a small number of patients. Jong revealed that one of 10 (10.0%) malignancies and 3 of 12 (25.0%) benign lesions with increasing enhancement, 4 of 10 (40.0%) and one of 12 (8.3%) with plateau enhancement, 3 of 10 (30.0%) and one of 12 (8.3%) with washout enhancement, 2 of 10 (20.0%) and 7 of 12 (58.3%) without enhancement. Excluding one case of interference due to motion artifacts, Dromain showed that 7 of 19 (36.8%) breast cancers with increasing enhancement, 4 of 19 (21.1%) with plateau enhancement, 4 of 19 (21.1%) with washout enhancement, and 4 of 19 (21.1%) with no enhancement. Deng evaluated the relative enhancements between early and late phases and reported the proportions of enhancement patterns in 44 benign lesions and 106 breast cancers, respectively, were 15.9% and 17.9% for elevated pattern, 2.3% and 12.3% for steady pattern, 9.1% and 62.3% for depressed pattern, and 72.7% and 7.5% for non-enhanced pattern. As to our findings, in 102 benign lesions and 43 malignancies, separately, ascending type accounted for 25.5% and 18.6%, steady type accounted for 16.7% and 27.9%, descending type accounted for 10.8% and 51.2%, and non-enhanced lesions accounted for 47.1% and 2.3%. No matter on MRI or CESM, malignant lesions had a tendency to demonstrate washout enhancement (depressed or descending patterns) and the majority of benign lesions showed non-enhanced or persistent enhancement (elevated or ascending patterns), which may be of great help to differentiate benign and malignant lesions.

Previously, Froeling *et al.*²⁰ had found a correlation of contrast agent kinetics between contrast-enhanced digital breast tomosynthesis and MRI, showing a moderate agreement ($k = 0.438$). Inspired by this, we compared the enhancement patterns between CESM and MRI and achieved a coincidence rate of 64.2% and moderate agreement ($k = 0.515$), which demonstrated that there was a certain consistency of enhancement patterns between two modalities.

So far, the order of image acquisition (CC prior to MLO or MLO prior to CC) on CESM was controversial²¹. In published papers, some exposed MLO views first^{11,16,22}, while others performed CC views first^{12,13}. In our CESM protocols, the sequence of CC or MLO position was not fixed. The distribution of enhancement patterns was not statistically different between CC prior to MLO and MLO prior to CC conditions in benign lesions, while the difference was significant in malignant lesions. So, it remained uncertain whether the projective order have effect on enhancement patterns.

One DCIS with no distinguishable enhancement is displayed in Fig. 3. Scattered microcalcifications in the left breast were detected on LE images. On subtractions images, there was a symmetrical moderate background parenchyma enhancement in bilateral breasts and no distinct enhancing area stronger than background enhancement was found. Contrast-enhanced MRI depicted non-mass enhancement with linear distribution in the left breast. The biopsy result of microcalcifications located in the left breast at 3 o'clock gave a diagnosis of atypical hyperplasia. Then the left mastectomy was performed and frozen section examination suggested multiple atypical hyperplasia in the left breast, and immunohistochemical analysis clarified DCIS. Accordingly, a comprehensive analysis combined with other examination results is necessary. The authors believe that not a single standard is all-powerful, and only make the most of complementary advantages of multiple modalities (such as mammography, ultrasound, MRI) can maximize the benefits to patients.

A major limitation of the current study was that sample size was insufficient, especially the malignant cases, and the diagnostic value of quantitative methods needs to be confirmed in a large-scale clinical experience. In addition, the number of cases in which MLO projected first was too small to determine whether the projection sequence affected enhancement pattern.

Finally, we come to the conclusion that enhancement intensity and patterns on CESM have relevance to pathological types of breast lesions and have good performances in the diagnosis of breast cancers. The enhancement intensity of malignancies was usually stronger than that of benign lesions. Besides, enhancement intensity may contribute to differentiate hormonal receptor status. In terms of enhancement patterns, a large proportion of malignant lesions have a tendency to demonstrate descending patterns and the majority of benign lesions show non-enhanced or ascending patterns. Moreover, CESM examinations show a moderate agreement on enhancement patterns with DCE-MRI. In conclusion, quantitative analysis of enhancement characteristics is feasible to the clinical practice on CESM.

Data availability

The datasets generated during and/or analysed during the current study are available from the corresponding author on reasonable request.

Received: 29 October 2019; Accepted: 11 May 2020;

Published online: 17 June 2020

References

- Li, T., Mello-Thoms, C. & Brennan, P. C. Descriptive epidemiology of breast cancer in China: incidence, mortality, survival and prevalence. *Breast Cancer Res Treat.* **159**, 395–406 (2016).
- Carney, P. A. *et al.* Individual and combined effects of age, breast density, and hormone replacement therapy use on the accuracy of screening mammography. *Ann Intern Med.* **138**, 168–175 (2003).
- Francescone, M. A. *et al.* Low energy mammogram obtained in contrast-enhanced digital mammography (CEDM) is comparable to routine full-field digital mammography (FFDM). *Eur J Radiol.* **83**, 1350–1355 (2014).
- Dromain, C. *et al.* Evaluation of tumor angiogenesis of breast carcinoma using contrast-enhanced digital mammography. *AJR Am J Roentgenol.* **187**, W528–537 (2006).
- Wessam, R., Gomaa, M. M., Fouad, M. A., Mokhtar, S. M. & Tohamy, Y. M. Added value of contrast -Enhanced Mammography in Assessment of Breast Asymmetries. *Br J Radiol.* **92**, 20180245 (2019).
- Lewin, J. M., Isaacs, P. K., Vance, V. & Larke, F. J. Dual-energy contrast-enhanced digital subtraction mammography: feasibility. *Radiology.* **229**, 261–268 (2003).

7. Cheung, Y. C. *et al.* Diagnostic performance of dual-energy contrast-enhanced subtracted mammography in dense breasts compared to mammography alone: interobserver blind-reading analysis. *Eur Radiol.* **24**, 2394–2403 (2014).
8. Mori, M. *et al.* Diagnostic accuracy of contrast-enhanced spectral mammography in comparison to conventional full-field digital mammography in a population of women with dense breasts. *Breast Cancer-Tokyo.* **24**, 104–110 (2017).
9. Sorin, V. *et al.* Contrast-enhanced spectral mammography in women with intermediate breast cancer risk and dense breasts. *AJR Am J Roentgenol.* **211**, W267–W274 (2018).
10. Fallenberg, E. M. *et al.* Contrast-enhanced spectral mammography vs. mammography and MRI - clinical performance in a multi-reader evaluation. *Eur Radiol.* **27**, 2752–2764 (2017).
11. Dromain, C. *et al.* Dual-energy contrast-enhanced digital mammography: initial clinical results. *Eur Radiol.* **21**, 565–574 (2011).
12. Rudnicki, W. *et al.* Correlation between quantitative assessment of contrast enhancement in contrast-enhanced spectral mammography (CESM) and histopathology-preliminary results. *Eur Radiol.* **29**, 6220–6226 (2019).
13. Deng, C. Y. *et al.* Quantitative analysis of enhanced malignant and benign lesions on contrast-enhanced spectral mammography. *Br J Radiol.* **91**, 20170605 (2018).
14. Luczynska, E. *et al.* Degree of enhancement on contrast enhanced spectral mammography (CESM) and lesion type on mammography (MG): comparison based on histological results. *Med Sci Monit.* **22**, 3886–3893 (2016).
15. Jong, R. A. *et al.* Contrast-enhanced digital mammography: initial clinical experience. *Radiology.* **228**, 842–850 (2003).
16. Fallenberg, E. M. *et al.* Contrast-enhanced spectral mammography versus MRI: Initial results in the detection of breast cancer and assessment of tumour size. *Eur Radiol.* **24**, 256–264 (2014).
17. Knogler, T. *et al.* Application of BI-RADS descriptors in contrast-enhanced dual-energy mammography: comparison with MRI. *Breast Care.* **12**, 212–216 (2017).
18. Marino, M. A. *et al.* Contrast-enhanced mammography and radiomics analysis for noninvasive breast cancer characterization: initial results. *Mol. Imaging Biol.* <https://doi.org/10.1007/s11307-019-01383-w> (2019).
19. Kuhl, C. K. *et al.* Dynamic breast MR imaging: Are signal intensity time course data useful for differential diagnosis of enhancing lesions? *Radiology.* **211**, 101–110 (1999).
20. Froeling, V. *et al.* Correlation of contrast agent kinetics between iodinated contrast-enhanced spectral tomosynthesis and gadolinium-enhanced MRI of breast lesions. *Eur Radiol.* **23**, 1528–1536 (2013).
21. Perry, H. *et al.* Contrast-enhanced mammography: a systematic guide to interpretation and reporting. *AJR. American journal of roentgenology.* **212**, 222–231 (2019).
22. Patel, B. K. *et al.* Clinical utility of contrast-enhanced spectral mammography as an adjunct for tomosynthesis-detected architectural distortion. *Clinical Imaging.* **46**, 44–52 (2017).

Acknowledgements

We thank Sichuan University West China Hospital for device support, and numerous individuals participated in this study.

Author contributions

Y.L., S.Z. and J.Q.Y. conceived and designed the study. X.Q.Z. performed examinations. J.H. and Y.Q. conducted image analysis. S.Z. and H.H.Z. collected data. Y.L. performed statistical analysis and drafted the manuscript. J.Q.Y. reviewed the manuscript. All authors read and approved the manuscript for submission.

Competing interests

The authors declare no competing interests.

Additional information

Correspondence and requests for materials should be addressed to J.Y.

Reprints and permissions information is available at www.nature.com/reprints.

Publisher's note Springer Nature remains neutral with regard to jurisdictional claims in published maps and institutional affiliations.



Open Access This article is licensed under a Creative Commons Attribution 4.0 International License, which permits use, sharing, adaptation, distribution and reproduction in any medium or format, as long as you give appropriate credit to the original author(s) and the source, provide a link to the Creative Commons license, and indicate if changes were made. The images or other third party material in this article are included in the article's Creative Commons license, unless indicated otherwise in a credit line to the material. If material is not included in the article's Creative Commons license and your intended use is not permitted by statutory regulation or exceeds the permitted use, you will need to obtain permission directly from the copyright holder. To view a copy of this license, visit <http://creativecommons.org/licenses/by/4.0/>.

© The Author(s) 2020